Numerical Analysis of the Stability of Soil Slope Subjected to Rainwater Infiltration

H. R. Bhanuprakash and Adarsh S. Chatra

1 Introduction

Slope failures and landslides are some of the major geological processes occurring frequently in the world. Landslides affect 15% of the land area of India. The term, 'landslide' is defined as the movement of a mass of a rock, debris or earth down a slope under the influence of gravity (Cruden [1]). The subject of stability analysis of rain-induced failures in soil is an interesting, important and challenging one in geotechnical engineering. The slope failures and landslides occur when hill slopes become mechanically unstable, because of geologic and hydrogeologic processes and pose a serious threat to human life and built environments. The process of rainwater infiltration into the soil and its movement in unsaturated soils has been studied by hydrologists, geologists and geotechnical engineers by carrying out field and numerical examinations [2–6]. The physics-based and numerical models are capable of reproducing the physical processes during rainfall intrusion and failure initiation in the variably saturated soils during the process of slope failures and subsequent mass movement. Landslides are also referred as landslips, slump or slope failure. These landslides not only cause extensive damage to the property but also cause loss of lives. The triggering factors responsible for landslides are rainfall, rapid snowmelt, earthquakes and anthropogenic activities.

Anderson and Pope [7] studied unsaturated flow into a hydrological model to investigate the stability of a typical slope in Hong Kong. The authors concluded that saturated permeability is not a constant value in the unsaturated zone and is the function of the degree of saturation. Collins and Znidarcic [8] investigated the failure mechanisms of slopes subjected to rainwater infiltration. Significant buildup of positive pore-water pressure in the soil due to the rise of groundwater leads to failure. Authors concluded that slope failure is mainly because of a reduction in shear strength

H. R. Bhanuprakash (✉) · A. S. Chatra
Basaveshwar Engineering College, Bagalkot 587102, India

33

of soil due to reduction in the magnitude of matric suction. Zhou et al. [9] investigated the effects of rainfall duration, rainfall intensity and soil weakening on stability of slope. Seepage-stress coupling model is used to examine an actual disastrous event in Yulin China. Authors conclude that the safety factor drops sharply at first and then gradually declines to 1.05 during additional two days of intense rainfall indicating the slope is at the verge of failure. Gidon and Sahoo [10] conducted numerous studies and used many innovative techniques to understand the problems due to slope instability under rainfall. The authors suggested that bamboos can be widely used as a reinforcement material for soil stabilization. The process of rainwater infiltration into the soil and its movement in unsaturated soils have been studied by several researchers by carrying out numerical simulations [3, 4, 11].

The study presented in this paper focuses on the relationship between the stability of soil slope and rainfall intensity and duration. The effects of hydraulic characteristics of soil, rainfall intensity and duration on the stability of soil slopes are studied in detail. The main rainfall events are applied to the slope right after the application of the antecedent rainfall. The antecedent rainfall is applied to simulate the initial conditions normal just before the occurrence of the major rainfall events. The variations in pore-water pressure in slopes under different rainfalls are calculated using Finite Difference Analysis (FDA) of transient water flow through unsaturated soils. These pore-water pressures are then used along with the strength reduction technique to calculate the Factor of Safety (FOS) using FDA. All the finite difference calculations have been performed using FLAC [12].

2 Slope Geometry and Boundary Conditions

In this study, the slope geometry mechanical and hydraulic properties are considered. Figure 1 shows the Finite Difference (FD) mesh of homogeneous slope having specific slope geometry and boundary conditions. The slope angle of 35°, slope height of 8 m and initial height of groundwater table from the bottom of the slope is taken as 6 m in the analysis. The boundary conditions were utilized for the seepage analysis. Along the sides of the slope below the water table, a boundary condition equal to the total head is applied.

3 Initial Conditions

First, an antecedent total rainfall of 2565.7 mm ($I = 8.133 \times 10^{-8}$ m/s) prior to the main rainfall event is applied to the surface of slope for 1 year in order to simulate the antecedent groundwater conditions in the slope section. The pore-water pressure, degree of saturation, shear strain, etc. are calculated at the end of the main rainfall events. The plots corresponding to the above response variables are drawn against
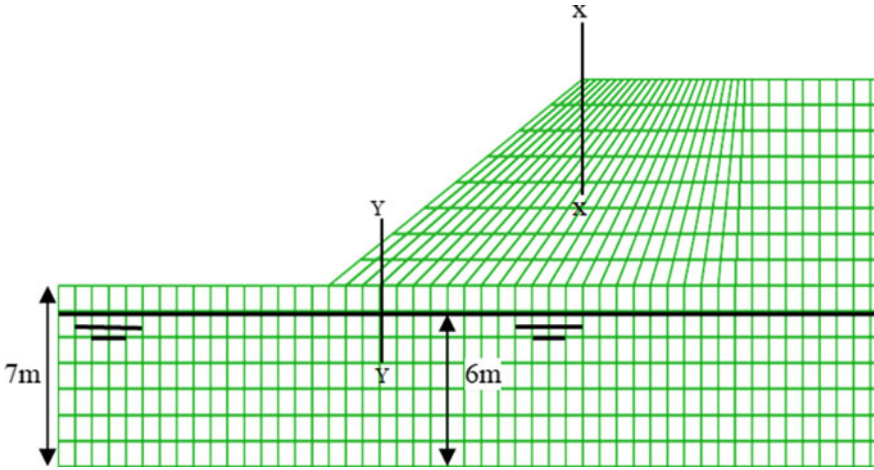
Fig. 1 Finite difference mesh of finite slope

the time from the slope surface at the selected locations in the top (Section x-x) and bottom (Section y-y) portion of the slope.

4 Soil Properties

For FDA, the slope section having the following soil properties is considered. The Mohr–Coulomb soil parameters and van Genuchten hydraulic parameters are given in Tables 1 and 2, respectively. The soil properties are considered to study the response slope subjected to main rainfall event. The rainfall is applied after the antecedent conditions created in the slope section. The properties of the soil types are given in Table 2, in which γ_d = dry unit weight, n = porosity, φ' = friction angle P_0 = Scaling suction m = Shape parameter and θ_r = Residual saturation.

Table 1 Soil parameters for Mohr–Coulomb model

Soil Property	Measured Value	Unit
Mechanical parameters		
Bulk modulus (K)	12.7	MPa
Shear modulus (G)	3.91	MPa
Effective cohesion	3.1	kPa
Effective friction angle	26	Degrees

Table 2 Mechanical and hydraulic properties of the soil.

Soil Property	Measured Value	Unit
Young's modulus (E)	10.7	MPa
Poisson's ratio (μ)	0.37	
Cohesion (c')	3.1	kPa
Shape parameter (m)	0.86	
Scaling suction (P_0)	9.81	kPa
Residual saturation (θ_r)	0.0954	

5   Results and Discussion

The typical rainfall intensities ($I = 4.05 \times 10^{-7}$, 1.39×10^{-6}, 1.119×10^{-6}, 1.10×10^{-6}, 1.38×10^{-6} m/s) are applied on the slope section to study the effects of rainfall intensities on the stability. Before the application of these main rainfall intensities, an antecedent rainfall of 2565.7 mm ($I = 8.133 \times 10^{-8}$ m/s) in 1-year period is applied over the slope section. The abovementioned rainfall intensities are applied over the homogeneous soil slope. The pore-water pressure at time, t = 0 h represents the pore-water pressure measured after the antecedent rainfall. After the application of main rainfall event, the increase in pore-water pressure is observed for the soil slopes. The results in the form of variations in pore-water pressure distribution, degree of saturation, shear strain increment at Sections x-x and y-y are provided.

5.1   Effect of Rainfall on Pore-Water Pressure Generation

An antecedent total rainfall of 2565.7 mm ($I = 8.133 \times 10^{-8}$ m/s) is applied to the slope section up to 1-year period in order to simulate the antecedent groundwater conditions prior to the main rainfall event. Figure 2a, b shows the evolution of pore-water pressures with rainfall duration. Figure 2a shows the variation of pore pressure at Section x–x. The variations in pore pressures at 1, 2 and 3 m depth are − 9.8, − 10.67 and − 8.4 kPa, respectively, at time t = 0 h. At time t = 120 h, the pore pressure values at 1, 2 and 3 m depth are − 0.77, 5.7 and 8.51 kPa, respectively. Figure 2b shows the variation of pore pressure at Section y–y. The pore pressure up to 48 h increases. Thereafter, the pore pressure remains constant.

5.2   Effect of Rainfall on the Stability of Slope

The changes in FOS values with rainfall duration for the slope sections are shown in Fig. 3. The rate of decrease in FOS values as the rainfall duration increases. For the slope section, a FOS of 1.41 is obtained at the end of antecedent rainfall duration
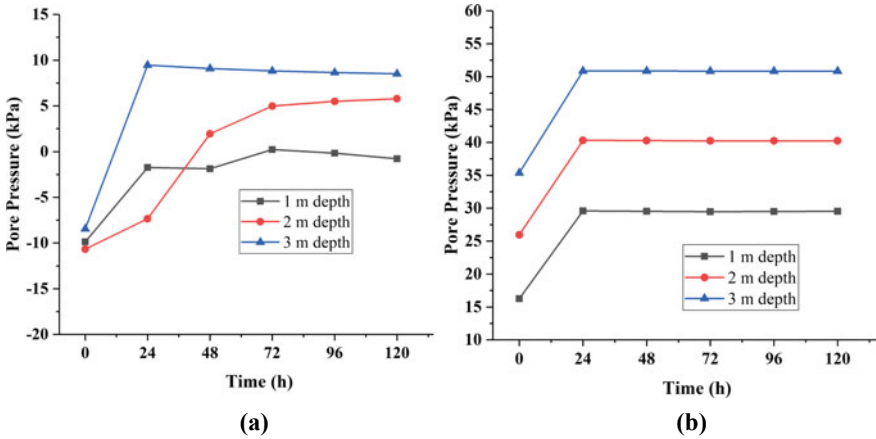
Fig. 2 (**a**) Variation of pore pressure at Section x-x and (**b**) Variation of pore pressure at Section y-y
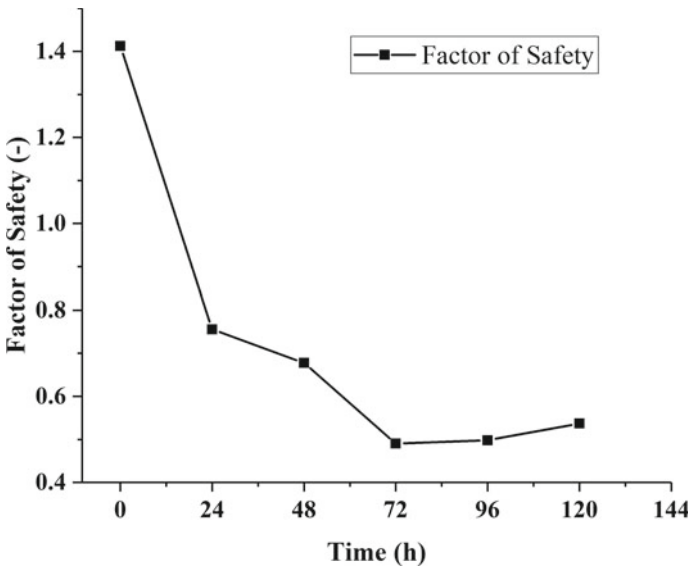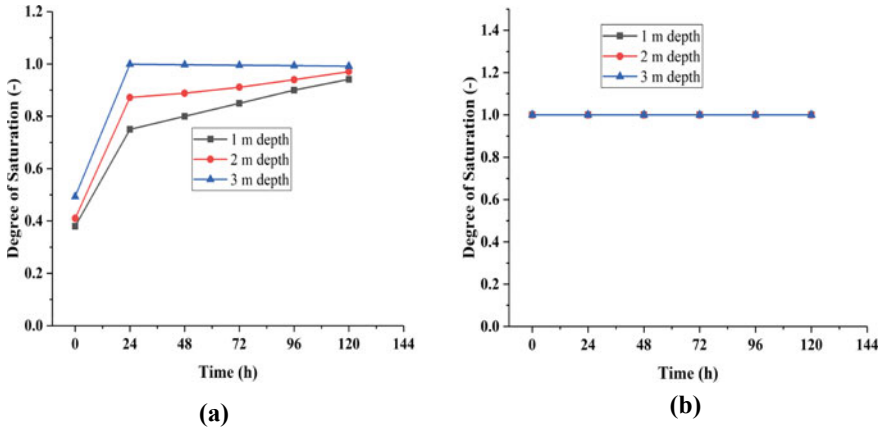

Fig. 3 Variation of factor of safety with time

(i.e. t = 0 h). The FOS values at time t = 18 h reduce to unity indicating slope is on the verge of failure. Further increase in rainfall duration the FOS values reduces less than unity indicating slope has failed. For the same slope with rainfall duration at time t = 120 h, i.e. end of rainfall the FOS value reduced to 0.537.

Fig. 4 (**a**) Variation of degree of saturation at Section x-x and (**b**) Variation of degree of saturation at Section y-y

## 5.3 Effect of Rainfall on Degree of Saturation

Figure 4a and b shows the variations of degree of saturation with time. Figure 4a shows the variation of degree of saturation at (Section x–x). At 1 m depth, the degree of saturation gradually increases. At 3 m depth, the degree of saturation increases from 49 to 100%, thereafter the degree of saturation remains constant. Figure 4(b) shows the variation of degree of saturation for (Section y–y). The rainwater infiltrated all along with the depth of the slope thereby fully saturating the slope.

5.4 Strain Response of Slope During Rainfall

The rainfall infiltration that leads to a decrease in matric suction also changes the shear strength and unit weight of the soil. The plots of shear strain increment with time are shown in Fig. 5a and b. Figure 5a depicts the variation of shear strain increment along (Section x-x). At 1, 2 and 3 m depths, the shear strain increment increases gradually. Figure 5b depicts the variation of shear strain increment along (Section y-y). The shear strain increment increases and thereafter remain constant.

6 Conclusions

The numerical simulations of rain-induced fluctuation are performed with finite difference method using FLAC. The effects of rain intrusion on the progressive slope
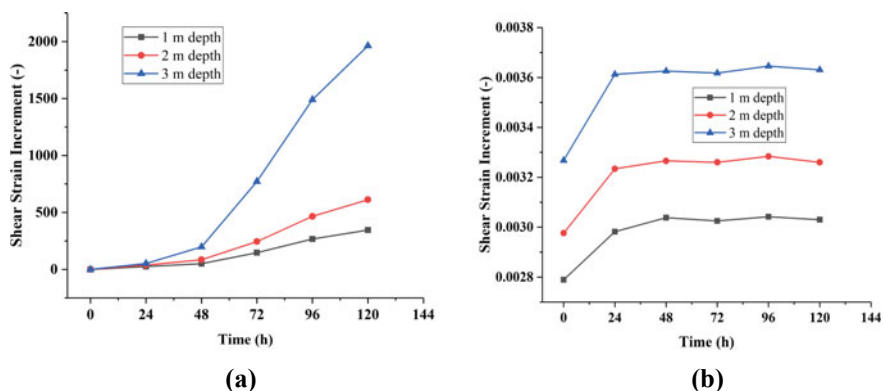
Fig. 5 (**a**) Variation of shear strain increment at Section x-x and (**b**) Variation of shear strain increment at Section y-y

deformations and the formation of a shear failure mechanism are studied. The rainfall intensities are applied over the slope right after the antecedent rainfall, which provided initial conditions for the stability analysis. The variations of pore-water pressure and FOS under these rainfall intensities are evaluated for the saturated–unsaturated slope section. The strain responses of the slopes are evaluated under rainfall intrusion. The numerical results of the present study have greater assurance in the practical stability analysis of the rain-induced earth slope instability. Actual rainfall data can be utilized in the simulation of pore pressure generation thereby giving instruction about the stability of the slope. Based on the results obtained for the selected slope section, soil properties and rainfall intensities, the following results are drawn:

1. During rainfall infiltration, the pore pressures increased due to the dissipation of matric suction and increase in the groundwater table corresponding to the antecedent conditions of the slope. For the slope, pore-water pressure increases for all the rainfall intensities.
2. For the slope section, a FOS of 1.41 is obtained at the end of antecedent rainfall duration. The FOS values at 18 h reduce to unity indicating the slope is unstable.
3. The degree of saturation decreases after the applied antecedent total rainfall and thereafter remains constant.
4. Shear strain values indicate that the soil first becomes unstable at the bottom then the instability extends to the top part of the slope.

References

1. Cruden, D.M.: A simple definition of landslide. Bull. Int. Assoc. Eng. Geol. 27–29 (1991)

2. Ali, A., Huang, J., Lyamin, A.V., Sloan, S.W., Cassidy, M.J.: Boundary effects of rainfall-induced landslides. Comput. Geotech. **61**, 341–354 (2014)
3. Cai, F., Ugai, K.: Numerical analysis of rainfall effects on slope stability. Int. J. Geomech. ASCE **4**(2), 69–78 (2004)
4. Chatra, A.S., Dodagoudar, G.R., Maji, V.B.: Numerical modelling of rainfall effects on the stability of soil slopes. Int. J. Geotech. Eng. **03**(5), 425–437 (2019)
5. Ng, C.W.W., Zhan, L.T., Bao, C.G., Fredlund, D.G., Gong, B.W.: Performance of an unsaturated expansive soil slope subjected to artificial rainfall infiltration. Geotechnique **53**(2), 143–157 (2003)
6. Tsaparas, I., Rahardjo, H., Toll, D.G., Leong, E.C.: Controlling parameters for rainfall-induced landslides. Comput. Geotech. **29**, 1–27 (2002)
7. Anderson, M.G., Pope, R.G.: The incorporation of soil water physics models in geotechnical studies of landslide behavior. In: Proceedings of the 4th International Symposium on Landslides, vol. 4, pp. 349–354 (1984)
8. Collins, B.D., Znidarcic, D.: Stability analyses of rainfall induced landslides. J. Geotech. Geoenviron. Eng. **130**(4), 362–372 (2004)
9. Zhou, D., Zhang, Z., Li, J., Wang, X.: Seepage-stress coupled modeling for rainfall induced loess landslide. Theor. Appl. Mech. Lett. **9**, 7–13 (2019)
10. Gidon, J.S., Sahoo, S.: Rainfall-induced slope failures and use of bamboo as a remedial measure: a review. Indian Geotechn. Soc. **50**, 766–783 (2020)
11. Rabie, M.: Comparison study between traditional and finite element methods for slopes under heavy rainfall. Hous. Build. Natl. Res. Center **10**, 160–168 (2014)
12. FLAC Flac Manual: Fluid-mechanical interaction. Itasca Consulting Group Inc., Minneapolis (2011)